

1 Epidemic dynamics shape inferences of the differences in
2 incubation-period and generation-interval distributions of the
3 Delta and Omicron variants
4

5 **Abstract**

6 Estimating the differences in the incubation-period and serial-interval distributions
7 of SARS-CoV-2 variants is critical to understanding changes in their transmission
8 dynamics and therefore controlling their outbreaks. However, these comparisons are
9 inherently difficult due to their dependence on epidemic growth rates—for example,
10 when an epidemic is growing exponentially, a cohort of infected individuals who
11 developed symptoms at the same time are more likely to have shorter incubation
12 periods. Here, we re-analyze incubation-period and serial-interval data collected by
13 Backer *et al.*, describing transmissions of the Delta and Omicron variants from
14 Netherlands at the end of December 2021. Previous analysis of the same data set
15 reported shorter mean observed incubation period (3.2 days vs 4.4 days) and serial
16 interval (3.5 days vs 4.1 days) for the Omicron variant, but the number of
17 infections caused by the Delta variant decreased during this period as the number
18 of Omicron infections increased. When we account for growth-rate differences of
19 two variants, we estimate similar mean incubation periods (3.8–4.5 days) for both
20 variants but a shorter mean generation interval for the Omicron variant (3.0 days;
21 95% CI: 2.7–3.2 days) than for the Delta variant (3.8 days; 95% CI: 3.7–4.0 days).
22 The differences in generation intervals may reflect higher reproduction numbers of
23 the Omicron variant, which can drive faster susceptible depletion among close
24 contacts. Neglecting differences in the generation-interval distributions can further
25 bias in estimates of the reproduction advantage of the Omicron variant.

1 Introduction

Estimating transmission advantages of new SARS-CoV-2 variants is critical to predicting and controlling the course of the ongoing COVID-19 pandemic. Transmission advantages of invading variants are typically characterized by the ratios of reproduction numbers, $\mathcal{R}_{\text{inv}}/\mathcal{R}_{\text{res}}$, and the differences in growth rates, $r_{\text{inv}} - r_{\text{res}}$. These two quantities are linked by the generation-interval distributions of the resident and invading variants. For example, an invading variant with shorter generation intervals—defined as the time between infection of the infector and the infectee—will exhibit faster epidemic growth ($r_{\text{inv}} > r_{\text{res}} > 0$) even if their reproduction numbers are identical ($\mathcal{R}_{\text{inv}} = \mathcal{R}_{\text{res}} > 1$).

Estimating generation-interval is hard, largely due to difficulties in observing actual infection events. Many researchers primarily focus on comparisons of other transmission intervals, such as time between symptom onsets (also referred to as serial intervals) or between testing events [1] of the infector and the infectee. However, transmission-interval distributions are subject to dynamical effects which can bias estimation. For example, when the epidemic is growing, a cohort of infectors who developed symptoms at the same time are more likely to have been infected recently, shortening their incubation periods—in other words, their incubation periods will be shorter, on average, than those of their infectees, causing the mean serial interval to be longer than the mean generation interval [2]. Therefore, observed differences in transmission-interval distributions between variants can give a biased picture of true differences in their generation-interval distributions, especially if their growth rates differ.

Here, we re-analyze serial-interval data collected by [3], representing within- and between-household transmissions of the Delta and Omicron variants from the Netherlands between 13 and 26 December 2021. The authors of the original article reported shorter serial intervals (3.5 vs 4.1 days) and incubation periods (3.2 vs 4.4 days) for transmission pairs with S-gene target failure (mostly omicron during the study period) and without (mostly delta), but did not consider growth-rate differences in their inference. Here, we discuss the epidemiological context in the Netherlands during the study period and take dynamics into account to provide corrected estimates for the incubation periods and generation-interval distributions of the Delta and Omicron variants.

2 Methods

2.1 Data

We analyze time series of reported COVID-19 cases (<https://data.rivm.nl/covid-19/>) and proportions of SARS-CoV-2 variants detected (<https://www.rivm.nl/coronavirus-covid-19/virus/varianten>) from the Netherlands between 29 November 2021 and 30 January 2022. Both data are publicly available on the National Institute for Public Health

65 and the Environment (RIVM) website.

66 Serial interval data are taken from the supplementary material of [3]. The data
67 are aggregated by the length of the serial interval in days and do not include addi-
68 tional individual-level information, such as exposure dates or symptom onset dates.
69 The data consists of 2529 transmission pairs and are further stratified by the pres-
70 ence of S gene target failure (SGTF), week of infectors’ symptom onset date (weeks
71 50 and 51), and the type of transmission (within or between households). In the
72 main text, we combine data from weeks 50 and 51 and instead present a stratified
73 analysis in Supplementary Material. For simplicity, we refer to transmission pairs
74 with and without SGTFs as Omicron and Delta transmission pairs, respectively. In-
75 cubation period data are not publicly available with the original article; instead, we
76 rely on previous estimates by [3] to derive growth-rate-adjusted incubation-period
77 distributions. See original article for details of data collection.

78 **2.2 Estimating epidemic growth rates**

79 To estimate the differences in growth rates of the Delta and Omicron variants, we
80 first estimate the number of COVID-19 cases caused by each variant by multiplying
81 reported weekly numbers of cases by the proportion of Delta and Omicron variants
82 detected—we use weekly time series to smooth over patterns of testing and reporting
83 within each week. We then fit a generalized additive model [4] to the logged weekly
84 case estimates to obtain smooth trajectories for case time series. Finally, we take the
85 derivative of the predicted logged numbers of cases caused by each variant to obtain
86 time-varying growth rate estimates.

87 To obtain confidence intervals on the estimated time-varying growth rates, we
88 generate 1000 parameter sets by resampling spline coefficients from a multivariate
89 normal distribution using the estimated variance-covariance matrices. We calculate
90 time-varying growth rates from each parameter set and use equi-tailed quantiles to
91 generate 95% confidence limits.

92 **2.3 Estimating forward incubation-period distributions from** 93 **backward incubation-period distributions**

94 [3] estimated the incubation periods from 513 individuals (258 Omicron and 255 Delta
95 cases), with symptom onsets between 1 December 2021 and 2 January 2022. They
96 used the methods of [5], which estimates incubation period by inferring distributions
97 of time of infection for each individual from their known exposure dates, using a
98 uniform distribution, and compares this to a known symptom-onset time.

99 In practice, incubation periods (and other epidemiological delays) can be mea-
100 sured in two ways: forward and backward. The forward incubation periods are
101 measured from a cohort of individuals who were infected at the same time. We ex-
102 pect this forward incubation-period distribution $f_I(\tau)$ to remain constant over the

course of an epidemic and provide reliable estimates of the distribution across individuals. Backward incubation periods are measured from a cohort of individuals who developed symptoms at the same time. We expect the backward incubation-period distribution to be sensitive to epidemic dynamics. The difference arises because forward incubation periods look forward from the reference point towards symptom development, which is an individual-level process, while backward incubation periods look backwards towards an infection event, which requires an interaction with an infectious individual.

In particular, when incidence of infection is growing exponentially, we are more likely to observe shorter backward incubation periods because there will be relatively more individuals who were infected recently. Assuming that incidence is changing exponentially at a constant rate r across the study period, the backward incubation-period distribution $b_I(\tau)$ corresponds to:

$$b_I(\tau) = \frac{\exp(-r\tau)f_I(\tau)}{\int_0^\infty \exp(-rx)f_I(x) dx}. \quad (1)$$

The method of [5] starts from observed symptom onsets, and estimates the backward incubation-period distribution without taking growth rates into account.

For a given growth rate r , the corresponding forward incubation-period distributions can be calculated by inverting Eq. (1):

$$f_I(\tau) = \frac{\exp(r\tau)b_I(\tau)}{\int_0^\infty \exp(rx)b_I(x) dx}. \quad (2)$$

Since incubation-period data are not provided, we are not able to fit Eq. (2) directly; instead we take the backward incubation-period distributions $b_I(x)$ estimated by [3], which was originally assumed to follow a Weibull distribution, and apply Eq. (2). In particular, [3] estimated the scale and shape parameters of the Weibull distribution to be 4.93 (95% CI: 4.51–5.37) and 1.83 (95% CI: 1.59–2.08), respectively, for the non-SGTF cases, and 3.60 (95% CI: 3.23–3.98) and 1.50 ((95% CI: 1.32–1.70), respectively, for SGTF cases.

We also model the backward incubation-period distribution $b_I(\tau)$ using a Weibull distribution based on the assumptions of [3]. To account for uncertainties in the original parameter estimates, we rely on a sampling scheme, similar to the one we used for the growth rate analysis (in Section 2.2). First, we approximate the previously inferred posterior distributions of the shape and scale parameters of the Weibull distribution using a lognormal distribution—we parameterize the lognormal distribution such that (i) its median matches the median of the posterior distributions and (ii) the probability that a random variable following the specified lognormal distribution falls between the lower and upper credible limits matches 95% [6]. We draw 1000 samples of the shape and scale parameters (for the backward distribution $b_I(\tau)$) from the specified lognormal distributions and estimate the corresponding forward distribution using Eq. (2). We take 95% equi-tailed quantiles to obtain 95% confi-

dence intervals. We repeat the analysis across plausible ranges of r for the Delta and Omicron variants separately (discussed later).

2.4 Estimating forward generation-interval distributions from forward serial-interval distributions

Dynamical biases in the serial-interval distributions are more complex because the serial interval depends on the incubation periods of the infector and the infectee as well as the generation interval between them (Fig. 1). For example, [3] measured the forward serial-interval distributions from cohorts of infectors who developed symptoms during the same week. In this case, the forward serial interval τ_s can be expressed in the form [2]:

$$\tau_s = -\tau_{i,1} + \tau_{g,\text{symp}} + \tau_{i,2}, \quad (3)$$

where $\tau_{i,1}$ represents the backward incubation period of the infector (because all infectors developed symptoms at the same time), and $\tau_{i,2}$, represents the forward incubation period of the infectee. Here, $\tau_{g,\text{symp}}$ represents the generation interval between the infector and the infectee; we use the subscript *symp* to indicate that these generation intervals are measured from infectors who developed symptoms at the same time.

The symptom-based generation-interval distribution describing Eq. (3) gives a biased picture because infectors who developed symptoms at the same time will have shorter incubation periods (when epidemic is growing) and therefore transmit earlier (Fig. 1A). This symptom-based generation-interval distribution depends on the backward incubation-period distribution:

$$f_{G,\text{symp}}(\tau) = \int_0^\infty f_{G|I}(\tau|x) b_I(x) dx, \quad (4)$$

where $f_{G|I}(\tau|x)$ represents the forward generation-interval distribution conditional on a known value of the incubation period, x . Instead, the forward generation-interval distribution measured from a cohort of individuals who were infected at the time is expected to provide reliable estimates of the distribution across individuals (because their incubation-period distribution is expected to remain constant over time, Fig. 1B):

$$f_{G,\text{inf}}(\tau) = \int_0^\infty f_{G|I}(\tau|x) f_I(x) dx. \quad (5)$$

When epidemic is growing is exponentially, we have two opposing effects affecting the relationship between the mean serial and generation interval. First, infectors in a given cohort are more likely to have shorter incubation periods than their infectees on average, $\mathbb{E}[\tau_{i,1}] < \mathbb{E}[\tau_{i,2}]$, causing the mean forward serial interval to be longer than the mean symptom-based generation interval ($\mathbb{E}[\tau_s] > \mathbb{E}[\tau_{g,\text{symp}}]$). Second, the

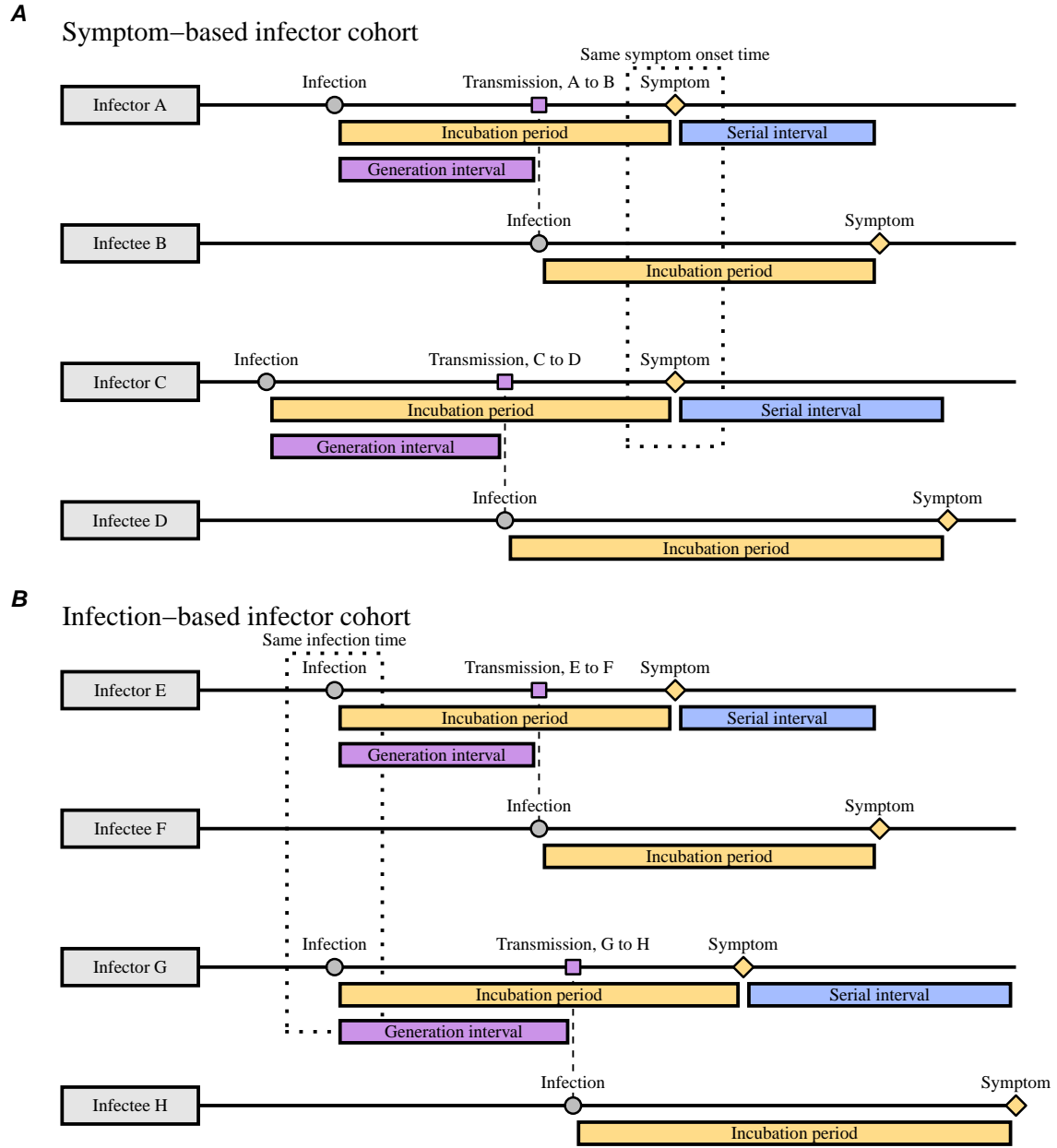


Figure 1: **Schematic diagrams of serial and generation intervals from symptom- and infection-based infector cohorts.** (A) Serial intervals are typically measured from the cohort of infectors who develop symptoms at the same time. In this case, infectors will have shorter incubation periods than their infectees on average; the corresponding generation intervals will be also short because infectors with short incubation periods will transmit earlier. (B) Generation intervals are better measured from the cohort of infectors who are infected at the same time because their incubation periods will be unbiased.

mean symptom-based generation interval will be shorter than the mean infection-based generation interval: $E[\tau_{g,\text{inf}}] > \mathbb{E}[\tau_{g,\text{symp}}]$. Therefore, the difference between the mean serial interval and the mean infection-based generation interval is difficult to predict in general; in most cases, however, we expect the former effect to dominate, causing the mean serial interval to be longer than the mean infection-based generation interval: $\mathbb{E}[\tau_s] > E[\tau_{g,\text{inf}}]$ [2]. For simplicity, we will use the term “forward generation-interval” to refer to the infection-based generation-interval distribution (measured from a cohort of infectors who were infected at the same infection time, Fig. 1B), and drop the subscript inf.

We model the forward incubation-period $f_I(\tau)$ and generation-interval $f_G(\tau)$ distributions using a bivariate lognormal distribution. The joint distribution is parameterized by log means, μ_I and μ_G , log variances, σ_I^2 and σ_G^2 , and the correlation coefficient on a log scale ρ . Thus, the forward generation-interval distribution conditional on the incubation period $f_{G|I}(\tau|\tau_{i,1})$ has a log mean of $\mu_G + \sigma_G\rho(\log(\tau_{i,1}) - \mu_I)/\sigma_I$ and a log variance of $\sigma_G^2(1 - \rho^2)$. Assuming that the incidence of infection is changing exponentially at rate r , the forward serial-interval distribution $f_S(\tau)$ for a cohort of infectors who developed symptoms at time $t = 0$ can be calculated by integrating across infection time of the infector $\alpha_1 < 0$ and of the infectee $\alpha_2 > \alpha_1$ [2]:

$$f_S(\tau) = \frac{1}{\phi} \int_{-\infty}^0 \int_{\alpha_1}^{\tau} \exp(r\alpha_1) f_{G|I}(\alpha_2 - \alpha_1 | -\alpha_1) f_I(-\alpha_1) f_I(\tau - \alpha_2) d\alpha_2 d\alpha_1, \quad (6)$$

where ϕ is a normalization constant chosen so that $\int f_S(x) dx = 1$; $-\alpha_1$ corresponds to the incubation period of the infector; $\alpha_2 - \alpha_1$ corresponds to the generation interval; and $\tau - \alpha_2$ corresponds to the incubation period of the infectee. As discussed earlier in Section 2.3, this method assumes that the incidence is changing exponentially at a constant rate r across the study period. As we show later in the results section, the exponential growth rate changes over the study period, including weeks 50 and 51; for illustrative purpose, we choose values of r that represent the dynamics of Delta and Omicron infections during this period and repeat the analysis across plausible ranges of r (discussed later in detail).

For a given value of r , we first estimate the forward incubation-period distribution from the backward distribution, previously estimated by [3], using Eq. (2). We then approximate the forward incubation-period distribution with a lognormal distribution by matching the mean and standard deviation. Using this incubation-period distribution, we fit Eq. (6) to the observed serial-interval data by minimizing the negative log-likelihood. We then calculate the mean forward generation interval using Eq. (5) and approximate the 95% confidence interval using the Delta method. We assume $\rho = 0.75$ throughout based on [7]—since we do not have individual-level data on infection and symptom onset times, we expect this parameter to be unidentifiable in practice. In Supplementary Material, we explore how assumptions about ρ affect inferences of the generation-interval distribution.

2.5 Estimating instantaneous reproduction number

We use our estimates of the generation-interval distributions to infer instantaneous reproduction numbers $\mathcal{R}(t)$ of the Delta and Omicron variant, as well as the ratio between two reproduction numbers. Estimating the instantaneous reproduction number—defined as the average number of secondary infections that a primary case will generate if epidemiological conditions remain constant [8]—requires the intrinsic generation-interval distribution $g(\tau)$:

$$\mathcal{R}(t) = \frac{i(t)}{\int_0^\infty i(t-x)g(x) dx}, \quad (7)$$

where $i(t)$ represents incidence of infection. Here, we approximate the intrinsic generation-interval distribution with the forward generation-interval that we estimate for week 50—when epidemic is growing or decaying exponentially, we expect the forward generation-interval to be a good proxy for the intrinsic generation-interval distribution [9, 10]. Incidence of infection is approximated by shifting the smoothed case trajectories by one week to account for reporting delays. This method of approximating incidence of infection assumes a fixed delay between infection and case reporting; in practice, deconvolution is required to accurately estimate the incidence of infection [11]. Case reports are also sensitive to changes in testing behavior, and therefore our estimates of $\mathcal{R}(t)$ must be interpreted with care. Confidence intervals are calculated by sampling parameters of the smoothed case trajectories as well as the generation-interval distributions from multivariate normal distributions and repeating the analysis 1000 times.

3 Results

Fig. 2 summarizes the epidemiological context in the Netherlands during the study period. The first known Omicron case in the Netherlands was sampled on 19 November 2021 [3], during a period when COVID-19 incidence was decreasing (Fig. 2A). As the Omicron variant continued to spread and increase in proportion (Fig. 2B), the number of COVID-19 cases started to increase (Fig. 2A). Multiplying the proportion of each variant with the number of reported COVID-19 cases further allows us to estimate the epidemiological dynamics of each (Fig. 2C). The number of COVID-19 cases caused by the Delta variant continued to decrease throughout the study period with time-varying growth rates decreasing from $r \approx -0.01/\text{day}$ to $r \approx -0.09/\text{day}$ by the week of January 16, 2022, and increasing back up to $r \approx -0.04/\text{day}$ by the end of January, 2022. The number of COVID-19 cases caused by the Omicron variant increased rapidly but decelerated over time with time-varying growth rates decreasing from $r = 0.18/\text{day}$ on the week of December 19, 2021, to $r = 0.04/\text{day}$ by the end of January, 2022. Finally, we find that the growth-rate difference between the Delta and Omicron variants decreased over time. Hereafter, we choose $r = -0.05/\text{day}$ for the Delta variant and $r = 0.15/\text{day}$ for the Omicron variant as our nominal growth

235 rates—these growth rates correspond to the mean growth rates between 1 December
 236 2021 and 2 January 2022, during which the incubation-period data were collected.
 237 We then evaluate the growth-rate effects across $r = -0.1/\text{day}$ – $0.0/\text{day}$ for the Delta
 238 variant and $r = 0.1/\text{day}$ – $0.2/\text{day}$ for the Omicron variant as a sensitivity analysis.

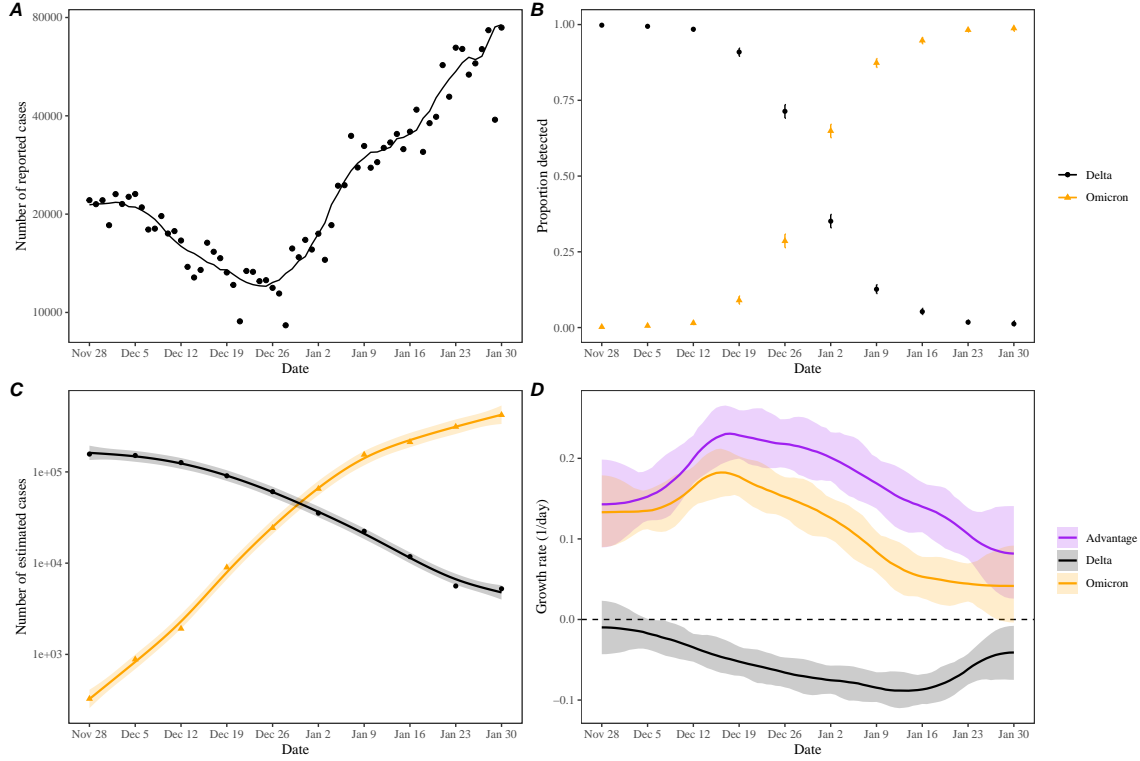


Figure 2: **Epidemic dynamics on the Delta and Omicron variants in the Netherlands.** (A) Daily numbers of reported COVID-19 cases in the Netherlands (points). The solid line represents the 7-day moving average. Data are publicly available on <https://data.rivm.nl/covid-19/>. (B) Proportion of SARS-CoV-2 variants detected from the Netherlands. Data are publicly available on <https://www.rivm.nl/coronavirus-covid-19/virus/varianten>. (C) Weekly numbers of COVID-19 cases caused by the Delta (black points) and Omicron (orange triangles) variants are estimated by multiplying the weekly numbers of cases (A) with the proportion of each variant (B). Solid lines and shaded areas represent fitted lines and corresponding 95% confidence intervals using generalized additive model. (D) Estimated growth rates of the Delta (black) and Omicron variants (orange) and their growth-rate differences (purple). Lines and shaded areas represent medians and corresponding 95% confidence intervals. Growth rates are estimated by taking the derivative of the generalized additive model estimates.

239 For a cohort of individuals who developed symptoms between 1 December 2021
 240 and 2 January 2022, [3] found longer mean (backward) incubation period for the
 241 Delta variant than for the Omicron variant (Fig. 3A). However, these measurements

242 were done during a period when the incidence of Omicron was increasing while the
 243 increasing of Delta was decreasing (Fig. 2). Thus, dynamical bias would be expected
 244 to lead to shorter observed (backward) incubation periods in Omicron, and longer
 245 observed incubation periods in Delta. When we account for these growth-rate dif-
 246 ferences and re-estimate the forward incubation periods, we find that both variants
 247 have similar incubation-period distributions (Fig. 3B)—for illustrative purposes, we
 248 assume $r = -0.05/\text{day}$ and $r = 0.15/\text{day}$ for the Delta and Omicron variants, re-
 249 spectively. Although the exact estimate of the mean forward incubation periods of
 250 both variants are sensitive to the assumed growth/decay rates, we find similar means
 251 across a plausible ranges of growth rates with unclear differences between two vari-
 252 ants (Fig. 3C–D). For example, the mean forward incubation period of the Delta
 253 variant changes from 3.8 days (95% CI: 3.5–4.1 days) to 4.4 days (95% CI: 4.0–4.8
 254 days) as we change the assumed values of r from $-0.1/\text{days}$ to $0/\text{days}$ (Fig. 3C),
 255 while the mean forward incubation period of the Omicron variant changes from 3.8
 256 days (95% CI: 3.4–4.4 days) to 4.5 days (95% CI: 3.9–5.5 days) as we change the
 257 assumed values of r from $0.1/\text{days}$ to $0.2/\text{days}$ (Fig. 3D).

258 Our corrected estimates of the forward incubation-period distributions further
 259 allow us to infer the forward generation-interval distributions. For illustrative pur-
 260 poses, we first focus on aggregated serial intervals from infectors who developed
 261 symptoms during week 50–51 (13–19 December, 2021). For within-household trans-
 262 mission pairs (Fig. 4A), the Omicron variant has shorter mean serial interval (3.1
 263 days; 95% CI: 2.9–3.3 days) than that of the Delta variant (3.7 days; 95% CI: 3.5–3.8
 264 days). When we account for growth-rate differences (assuming $r = -0.05/\text{day}$ and
 265 $r = 0.15/\text{day}$ for the Delta and Omicron variants, respectively), the estimated mean
 266 forward generation interval exhibits a slightly larger difference (Fig. 4B): 3.0 days
 267 (95% CI: 2.7–3.2 days) for the Omicron variant and 3.8 days (95% CI: 3.7–4.0 days)
 268 for the Delta variant. Across plausible ranges of assumptions about the growth rates
 269 of the Delta and Omicron variants, we estimate robust differences in their mean
 270 generation intervals (Fig. 4C–D). Assuming lower values of the correlation between
 271 the incubation period and generation intervals leads to larger differences in the mean
 272 generation intervals of the Delta and Omicron variants (Supplementary Figure S1).

273 Similar pictures arise for between-household transmission pairs, but the differ-
 274 ence in mean serial intervals are unclear (Fig. 4E): 3.0 days (95% CI: 2.7–3.3 days)
 275 for the Omicron variant and 3.3 days (95% CI: 3.0 days–3.6 days) for the Delta
 276 variant. Consistent with the original study, which also reported shorter mean serial
 277 intervals for between-household pairs [3], we estimate shorter mean generation in-
 278 tervals for between-household Delta pairs. While the difference in mean generation
 279 intervals is larger, there is greater uncertainty in their mean estimates (Fig. 4F): 2.9
 280 days (95% CI: 2.5–3.3 days) for the Omicron variant and 3.5 days (95% CI: 3.2–3.8
 281 days) for the Delta variant. Once again, these patterns are robust across plausible
 282 ranges of assumptions about the growth rates of the Delta and Omicron variants
 283 (Fig. 4G–H).

284 In Supplementary Figure S2, we present generation-interval estimates that are

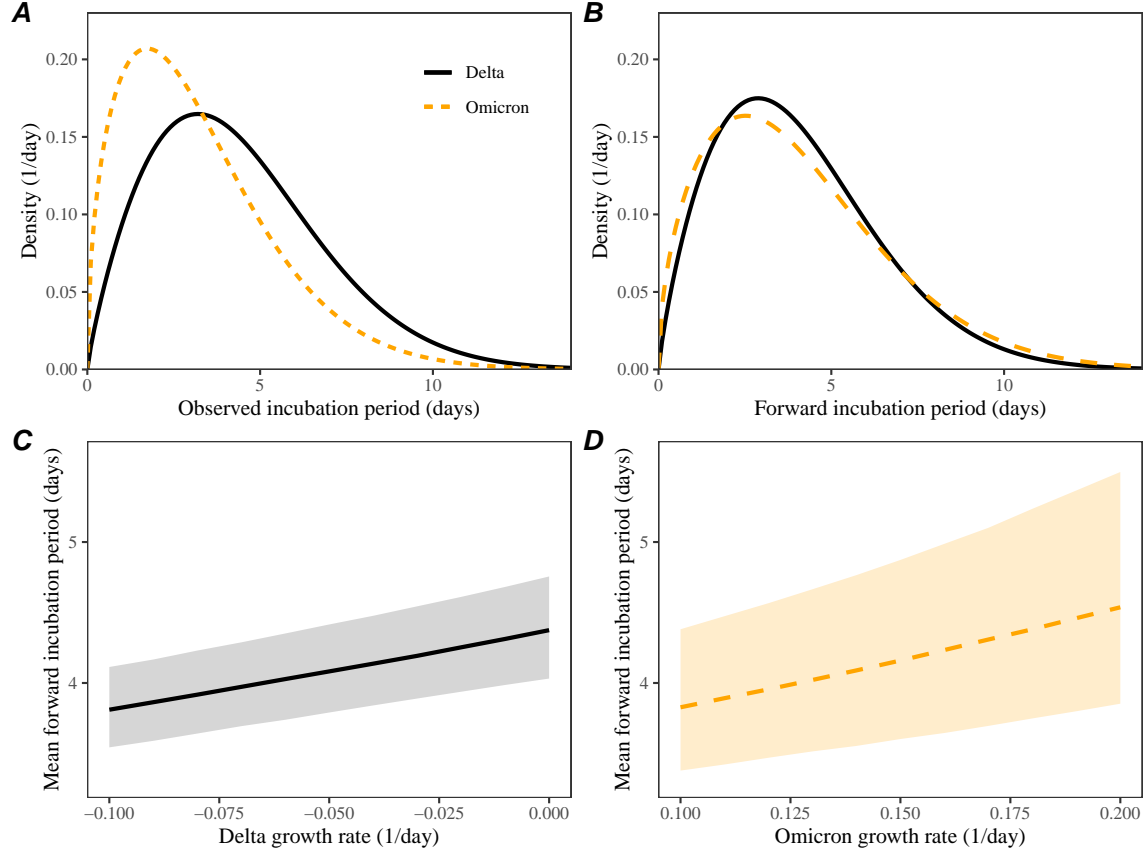


Figure 3: Observed and corrected differences in incubation-period distributions of Delta and Omicron variants. (A) Posterior median estimates of the observed (backward) incubation periods of the Delta (black) and Omicron (orange) variants by [3]. (B) Forward incubation-period distributions assuming $r = -0.05/\text{day}$ and $r = 0.15/\text{day}$ for the Delta (black) and Omicron (orange) variants, respectively. (C–D) Corrected estimates of the mean forward incubation-period for different assumptions about the growth rates of the Delta (C) and Omicron variants (D). Lines represent median estimates. Shaded regions represent the corresponding 95% confidence intervals.

285 further stratified by the week of infectors’ symptom onset (weeks 50 and 51). While
 286 we generally estimate shorter mean generation intervals for the Omicron variant,
 287 but the differences are unclear across all stratification, except for within-household
 288 transmission pairs during week 50. We also estimate a reduction in the mean forward
 289 generation intervals from week 50 to week 51 (especially for the Delta variant).

290 Accounting for differences in the generation-interval distributions, we estimate
 291 that the reproduction number of the Omicron variant decreased from 1.73 (95% CI:
 292 1.59–1.89) to 1.14 (95% CI: 1.00–1.32) between December 12, 2021, and January
 293 23, 2022 (Fig. 5A). On the other hand, the reproduction number of the Delta vari-
 294 ant decreased from 0.90 (95% CI: 0.83–0.97) to 0.69 (95% CI: 0.65–0.75) between

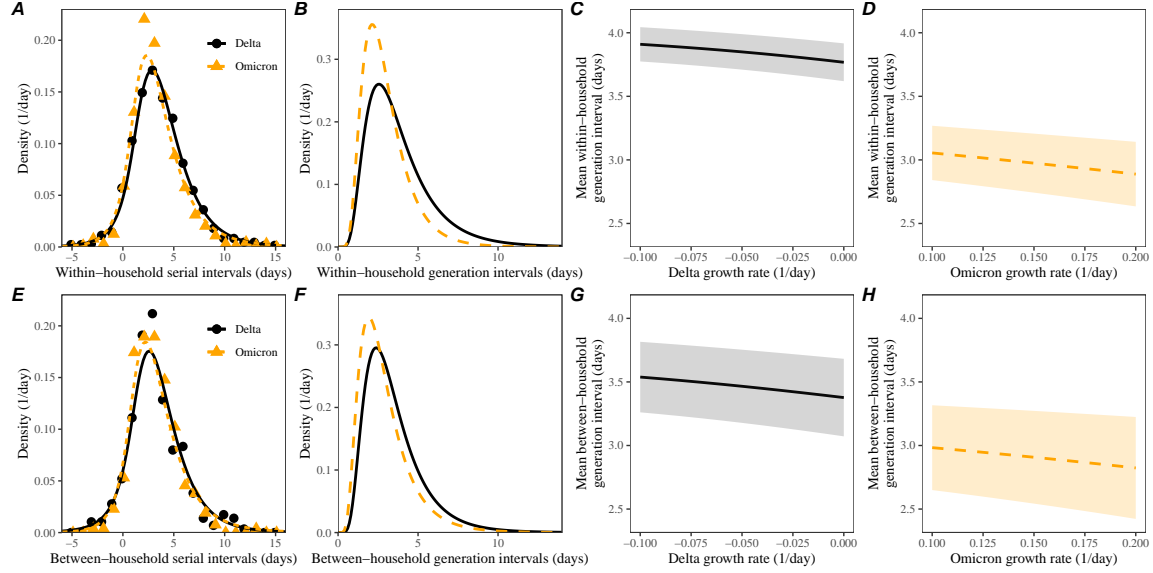


Figure 4: Estimated forward generation-interval distributions of Delta and Omicron variants. (A, E) Observed and fitted forward serial-interval distributions for within-household (A) and between-household (E) transmission pairs in the Netherlands for the Delta (black) and Omicron (orange) variants [3]. Serial intervals are calculated for infectors who developed symptoms on weeks 50 and 51 (13–26 December, 2021). Points represent the observed data. Lines represent the fitted lines assuming $r = -0.05/\text{day}$ for the Delta variant and $r = 0.15/\text{day}$ for the Omicron variant. (B, F) Estimated forward generation-interval distributions for within-household (B) and between-household (F) transmission pairs in the Netherlands. (C, D, G, H) Sensitivity of the mean forward generation-interval estimates to assumed growth rates of the Delta (C, G) and Omicron variants (G, H) for within-household (C, D) and between-household (G, H) transmission pairs. Lines represent median estimates. Shaded regions represent the corresponding 95% confidence intervals.

December 5, 2021, and January 9, 2022, and increased back up to 0.83 (95% CI: 0.73–0.94) by January 23, 2022 (Fig. 5A). We estimate the reproduction number ratios stayed roughly constant at around 2.10 (95% CI: 1.90–2.33) between December 12–26, 2021, and slowly decreased to 1.38 (95% CI: 1.15–1.65). However, if we neglect differences in the generation-interval distributions and solely rely on the generation-interval-distribution estimate for the Delta variant, we over-estimate the reproduction number of the Omicron variant and therefore is transmission advantage (Fig. 5B). In this case, the reproduction ratio decreases from 2.38 (95% CI: 2.13–2.67) to 1.43 (95% CI: 1.17–1.75), corresponding to roughly 4–13% bias. Using between-household generation intervals also gives similar conclusions about changes and biases in the reproduction number estimates (Supplementary Figure S3).

In both cases, the decrease in the reproduction number ratio coincides with the

307 decrease in the reproduction number of the Omicron variant, implying that epidemi-
 308 ological changes driving the dynamic had larger effects on the transmission of the
 309 Omicron variant than on the transmission of Delta variant; a larger reduction in the
 310 reproduction number of the Omicron variant also caused its growth rate to decrease
 311 faster, causing changes in the growth-rate difference (Fig. 2D).

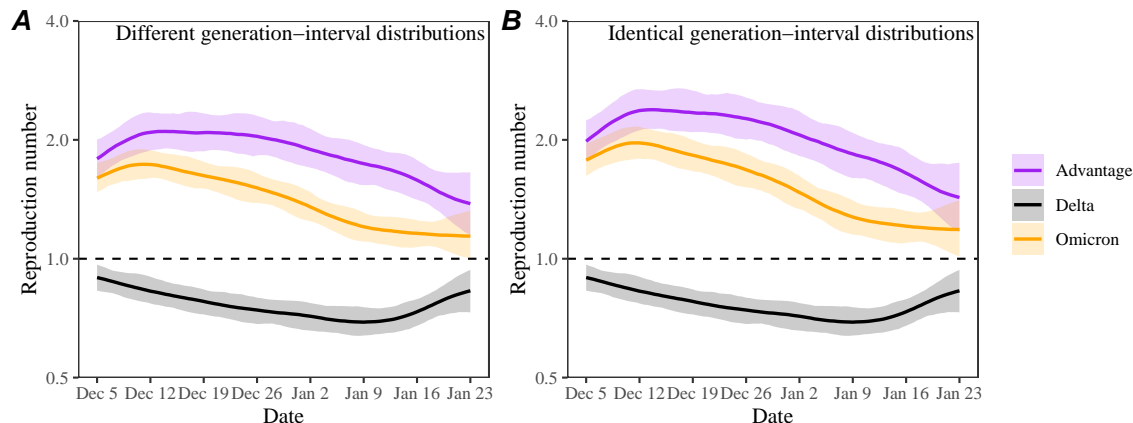


Figure 5: **Estimated time-varying reproduction number advantages of the Omicron variant.** (A) Estimated instantaneous reproduction numbers and their ratios over time while accounting for differences in the generation-interval distributions. (B) Estimated instantaneous reproduction numbers and their ratios over time while assuming identical generation-interval distributions. The instantaneous reproduction number of each variant is estimated using the renewal equation by shifting the smoothed case curves by one week (Fig. 2C). The intrinsic generation-interval distribution is approximated by the maximum likelihood estimates of the forward generation-interval distributions for within-household transmission pairs based on $r = -0.05$ for the Delta variant (black) and $r = 0.15$ for the Omicron variant (orange). Purple lines represent the ratio between the effective reproduction numbers of the Delta and Omicron variants. Lines and shaded regions represent medians and corresponding 95% confidence intervals.

312 4 Discussion

313 We compare estimates of the forward incubation-period and generation-interval dis-
 314 tributions of the Delta and Omicron variants from the Netherlands. The original
 315 analysis detailing the data set previously reported shorter mean incubation period
 316 and serial interval for the Omicron variant [3]. Accounting for differences in epidemic
 317 growth rates, we find similar incubation-period distributions for both variants but
 318 a shorter (0.3–0.8 days) mean generation interval for the Omicron variant. Finally,
 319 we estimate that the transmission advantage of the Omicron variant decreased from

2.1-fold to 1.4-fold between early December and late January. Neglecting differences in the generation-interval distributions can bias estimates of the transmission advantage.

The generation-interval distribution describes changes in the individual-level transmission dynamics over the course of infection and therefore provides crucial information for epidemic control. A few studies have estimated the generation-interval distributions of SARS-CoV-2 infections from serial-interval data, but most of them neglect the effects of epidemic growth rates [12, 13, 14, 15]—these practices can be largely attributed to historical work that concluded that serial and generation intervals have the same means based on the assumption that infectors and infectees have identical incubation-period distributions [16, 17, 18]. Here, we build on our previous work [2], which demonstrated theoretically that forward serial-interval distributions depends on epidemic growth rates, and further confirm that estimates of the forward generation-interval distributions are indeed sensitive to epidemic growth rates. Accounting for the growth-rate effects is especially important when comparing serial and generation intervals of different variants or from different time periods. These effects are also pertinent to all epidemiological inferences of past events from a cohort of infected individuals who experienced the succeeding event at the same time—this includes inferences of other delay distributions, such as incubation-period distributions, as well as viral load trajectories [19]. Our sensitivity analysis also shows that the assumptions about the correlation between incubation periods and generation intervals can also have important effects on the estimates of the generation-interval distributions (Supplementary Figure S1).

A few studies have suggested the the incubation period of the Omicron variant may be shorter than that of the Delta variant. The median estimates of the Omicron incubation period typically range between 3–4 days, consistent with earlier findings of [3]. However, these data were collected when the number of Omicron infections was growing rapidly [20, 21], suggesting that they may have been subject to similar biases. On the other hand, incubation-period estimates based on individuals who were exposed from the same event are likely more reliable (because they look forward in time): [22] estimated the median incubation period of the Omicron variant to be 3 days among those who attended the same holiday party ($n = 117$) on 26 November 2021 in Norway. However, we cannot rule out the possibility that some of these attendees were infected prior to the party given that some individuals had COVID-like symptoms prior to the party with at least 96 of the attendees sharing offices; neglecting these factors can lead to underestimation of the mean incubation period. Systematic comparisons of data collection methods and epidemiological contexts are needed to properly assess the differences in incubation period distributions of the Delta and Omicron variants.

To our knowledge, our study is the first to estimate the generation-interval distribution of the Omicron variant. Although we estimate a shorter mean generation interval for the Omicron variant, we find the generation-interval distribution of the Omicron and Delta variants have similar modes (around 2.5 days), implying that

the realized transmissibility of the Omicron variant decays faster. We tentatively hypothesize that these differences may be primarily driven by the network effect: a higher reproduction numbers of the Omicron variant leads to faster susceptible depletion among close contacts, which in turn prevents long generation intervals from generating infections [10, 15]. While the network effect is expected to be strongest among household contacts, it is also applicable to other forms of contact structures that involve repeated contacts between the same group of individuals (because only the first infectious contact results in infection). The network effect may also explain a decrease in the mean generation interval between week 50 and 51, especially among household transmission pairs, as a higher proportion of individuals within households would have been infected with either the Delta or Omicron variants. Shorter generation-interval estimates for between-household contacts may be attributable to behavioral effects: individuals who have symptoms or tested positive may be more likely to stay home, preventing long between-household transmission. Other factors, such as more stringent intervention measures against the Omicron variant [3] and shorter clearance phase of the Omicron variant [23], also likely contributed to shortening of the generation intervals.

While our study indicate that the Omicron variant has a shorter mean realized generation interval than that of the Delta variant, it is still uncertain how much their infectiousness profiles differ biologically. In particular, similarities in the incubation-period distributions of the Delta and Omicron variants suggest that the differences in their true infectiousness profile may be smaller than the estimated differences in their realized generation-interval distributions. In addition, the unmitigated generation intervals of both Omicron and Delta variants are likely longer than what we estimate given existing levels of interventions, including vaccination, and pandemic awareness—estimating “unmitigated” or “intrinsic” generation-interval distributions of SARS-CoV-2 variants are expected to be a difficult problem as it requires early data during which interventions and awareness levels were minimal [7]. Nonetheless, our estimates of the realized generation-interval distributions better describe the epidemic dynamics, implicitly accounting for intervention and behavioral effects, and are therefore should be used to estimate current reproduction numbers (rather than a counterfactual unmitigated generation-interval distribution, which may have a longer mean).

Our study also has important implications for estimating transmission advantages of new SARS-CoV-2 variants. In the example we consider, neglecting differences in the generation-interval distributions leads to $\approx 10\%$ bias in the estimates of the reproduction number ratios; however, the degree of ratio is expected to be sensitive to the assumed generation-interval distribution of the resident variant. For example, [24] estimated a much higher reproduction ratios (> 4 fold) in South Africa but also assumed a longer mean generation interval for the Delta and Omicron variants (6.4 vs 5.2 days, respectively). With our generation-interval estimates, we estimate that the reproduction number ratio of 2.6 assuming $r = -0.06$ and $r = 0.26$ for the Delta and Omicron variants, respectively—these growth rates were chosen to match the 4-fold

406 reproduction number ratios with the estimated growth-rate differences of 0.32/day
407 for the Gauteng province, South Africa [24]. We also show that both growth-rate dif-
408 ferences and the reproduction number ratios decreased over time—this result further
409 corroborates an earlier theoretical framework, which showed that growth-rate dif-
410 ferences change over the course of an epidemic even when the reproduction number
411 ratios remain constant [25].

412 We primarily rely on case data to understand epidemic patterns of the Delta and
413 Omicron variants. In doing so, we implicitly assume that the delay between infection
414 and reports is fixed. However, changes in case trajectories are sensitive to testing
415 patterns and therefore may not accurately reflect patterns of infections. While this
416 limitation does not affect our generation-interval estimates, our inferences of the
417 transmission advantages of the Omicron variant should be interpreted with care.

418 Monitoring changes in key epidemiological parameters is critical to understanding
419 the evolution of SARS-CoV-2 and predicting its future dynamics [26]. Our study syn-
420 thesises previously developed theoretical framework on serial- and generation-interval
421 distributions and presents methodological advances in monitoring epidemiological
422 parameters; however, uncertainty remains in the intrinsic infectiousness profiles of
423 SARS-CoV-2 variants, especially among asymptotically infected individuals [27].
424 Future studies extending our framework and combining more detailed epidemiologi-
425 cal data will be critical to narrowing down these uncertainties.

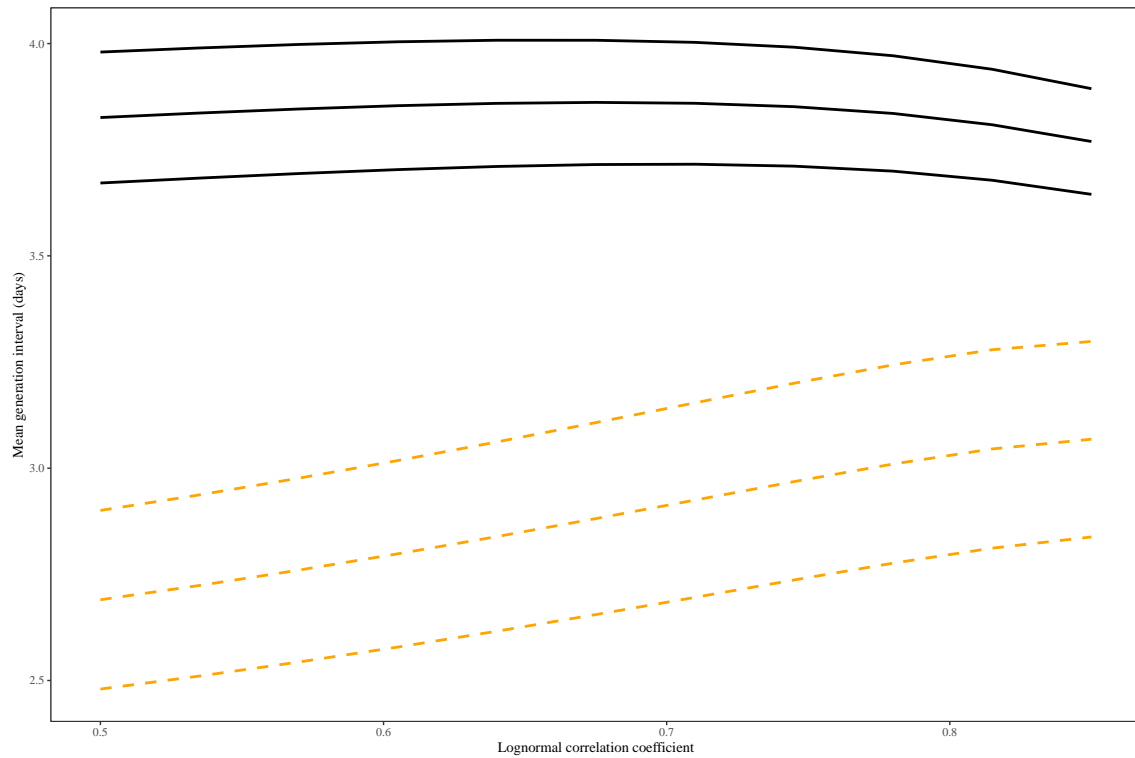


Figure S1: **Sensitivity of the estimates of the mean generation interval to the assumed values of the correlation coefficient of the lognormal distribution.** Lines represent maximum likelihood estimates and the corresponding 95% confidence intervals for the Delta (black, solid lines) and Omicron variants (orange, dashed lines). For illustrative purposes we use within-household serial-interval data from the cohort of infectors who developed symptoms during weeks 50 and 51.

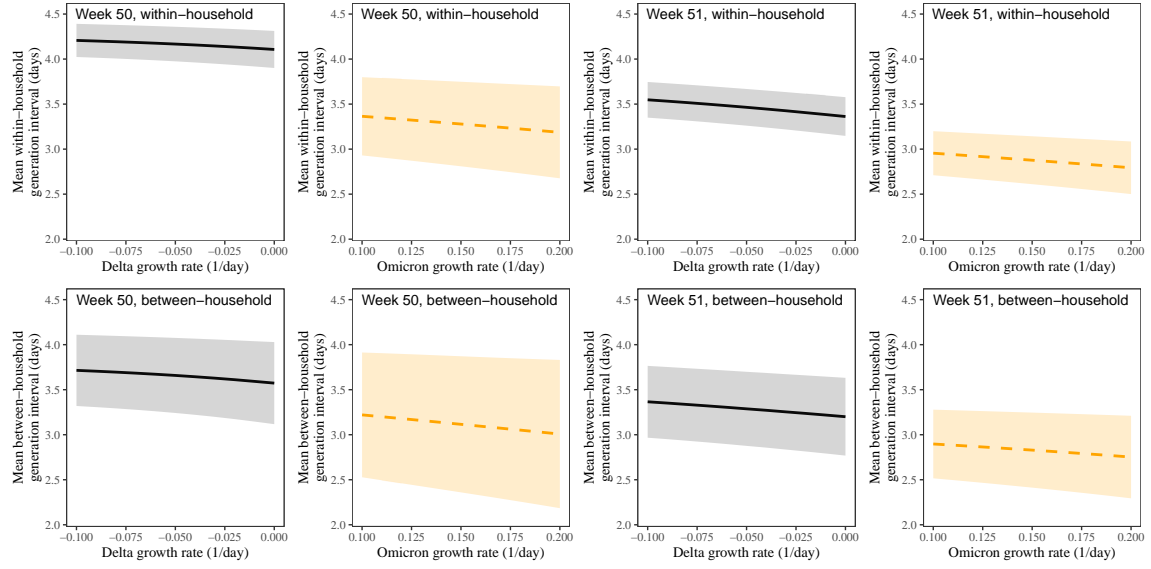


Figure S2: **Estimated mean forward generation intervals of Delta and Omicron variants across different stratifications.** See Figure 4 in the main text for figure caption.

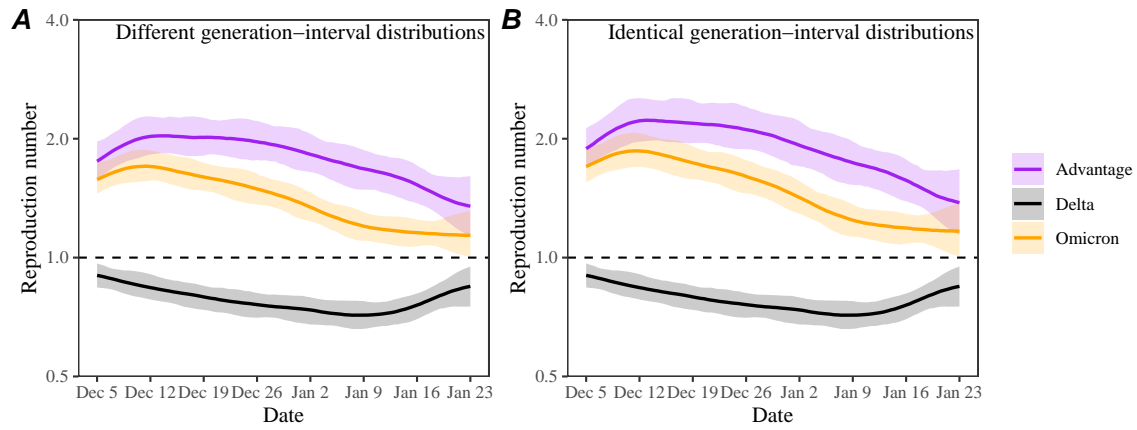


Figure S3: **Estimated time-varying reproduction number advantages of the Omicron variant using between-household generation-interval distributions.** See Figure 5 in the main text for figure caption.

References

- [1] Sam Abbott, Katharine Sherratt, Moritz Gerstung, and Sebastian Funk. Estimation of the test to test distribution as a proxy for generation interval distribution for the Omicron variant in England. *medRxiv*, 2022.
- [2] Sang Woo Park, Kaiyuan Sun, David Champredon, Michael Li, Benjamin M Bolker, David JD Earn, Joshua S Weitz, Bryan T Grenfell, and Jonathan Dushoff. Forward-looking serial intervals correctly link epidemic growth to reproduction numbers. *Proceedings of the National Academy of Sciences*, 118(2), 2021.
- [3] Jantien A Backer, Dirk Eggink, Stijn P Andeweg, Irene K Veldhuijzen, Noortje van Maarseveen, Klaas Vermaas, Boris Vlaemynck, Raf Schepers, Susan van den Hof, Chantal BEM Reusken, and Jacco Wallinga. Shorter serial intervals in SARS-CoV-2 cases with Omicron BA.1 variant compared with Delta variant, the Netherlands, 13 to 26 December 2021. *Eurosurveillance*, 27(6):2200042, 2022.
- [4] Simon N Wood. mgcv: GAMs and generalized ridge regression for R. *R News*, 1(2):20–25, 2001.
- [5] Jantien A Backer, Don Klinkenberg, and Jacco Wallinga. Incubation period of 2019 novel coronavirus (2019-nCoV) infections among travellers from Wuhan, China, 20–28 January 2020. *Eurosurveillance*, 25(5):2000062, 2020.
- [6] Sang Woo Park, Benjamin M Bolker, David Champredon, David JD Earn, Michael Li, Joshua S Weitz, Bryan T Grenfell, and Jonathan Dushoff. Reconciling early-outbreak estimates of the basic reproductive number and its uncertainty: framework and applications to the novel coronavirus (SARS-CoV-2) outbreak. *Journal of the Royal Society Interface*, 17(168):20200144, 2020.
- [7] Ron Sender, Yinon M Bar-On, Sang Woo Park, Elad Noor, Jonathan Dushoffd, and Ron Milo. The unmitigated profile of COVID-19 infectiousness. *medRxiv*, 2021.
- [8] Christophe Fraser. Estimating individual and household reproduction numbers in an emerging epidemic. *PloS one*, 2(8):e758, 2007.
- [9] David Champredon and Jonathan Dushoff. Intrinsic and realized generation intervals in infectious-disease transmission. *Proceedings of the Royal Society B: Biological Sciences*, 282(1821):20152026, 2015.
- [10] Sang Woo Park, David Champredon, and Jonathan Dushoff. Inferring generation-interval distributions from contact-tracing data. *Journal of the Royal Society Interface*, 17(167):20190719, 2020.

- [11] Edward Goldstein, Jonathan Dushoff, Junling Ma, Joshua B Plotkin, David JD Earn, and Marc Lipsitch. Reconstructing influenza incidence by deconvolution of daily mortality time series. *Proceedings of the National Academy of Sciences*, 106(51):21825–21829, 2009.
- [12] Tapiwa Ganyani, Cecile Kremer, Dongxuan Chen, Andrea Torneri, Christel Faes, Jacco Wallinga, and Niel Hens. Estimating the generation interval for coronavirus disease (COVID-19) based on symptom onset data, March 2020. *Eurosurveillance*, 25(17):2000257, 2020.
- [13] Xi He, Eric HY Lau, Peng Wu, Xilong Deng, Jian Wang, Xinxin Hao, Yiu Chung Lau, Jessica Y Wong, Yujuan Guan, Xinghua Tan, et al. Temporal dynamics in viral shedding and transmissibility of COVID-19. *Nature medicine*, 26(5):672–675, 2020.
- [14] Shi Zhao, Biao Tang, Salihu S Musa, Shujuan Ma, Jiayue Zhang, Minyan Zeng, Qingping Yun, Wei Guo, Yixiang Zheng, Zuyao Yang, et al. Estimating the generation interval and inferring the latent period of COVID-19 from the contact tracing data. *Epidemics*, 36:100482, 2021.
- [15] William S Hart, Elizabeth Miller, Nick J Andrews, Pauline Waight, Philip K Maini, Sebastian Funk, and Robin N Thompson. Generation time of the alpha and delta SARS-CoV-2 variants: an epidemiological analysis. *The Lancet Infectious Diseases*, 2022.
- [16] Åke Svensson. A note on generation times in epidemic models. *Mathematical biosciences*, 208(1):300–311, 2007.
- [17] Tom Britton and Gianpaolo Scalia Tomba. Estimation in emerging epidemics: biases and remedies. *Journal of the Royal Society Interface*, 16(150):20180670, 2019.
- [18] Sonja Lehtinen, Peter Ashcroft, and Sebastian Bonhoeffer. On the relationship between serial interval, infectiousness profile and generation time. *Journal of the Royal Society Interface*, 18(174):20200756, 2021.
- [19] James A Hay, Lee Kennedy-Shaffer, Sanjat Kanjilal, Niall J Lennon, Stacey B Gabriel, Marc Lipsitch, and Michael J Mina. Estimating epidemiologic dynamics from cross-sectional viral load distributions. *Science*, 373(6552):eabh0635, 2021.
- [20] Lauren Jansen, Bryan Tegomoh, Kate Lange, Kimberly Showalter, Jon Figliomeni, Baha Abdalhamid, Peter C Iwen, Joseph Fauver, Bryan Buss, and Matthew Donahue. Investigation of a Sars-Cov-2 B.1.1.529 (Omicron) variant cluster—Nebraska, November–December 2021. *Morbidity and Mortality Weekly Report*, 70(5152):1782, 2021.

- 499 [21] Jin Su Song, Jihee Lee, Miyoung Kim, Hyeong Seop Jeong, Moon Su Kim,
500 Seong Gon Kim, Han Na Yoo, Ji Joo Lee, Hye Young Lee, Sang-Eun Lee, et al.
501 Serial intervals and household transmission of SARS-CoV-2 Omicron variant,
502 South Korea, 2021. *Emerging Infectious Diseases*, 28(3):756, 2022.
- 503 [22] Lin T Brandal, Emily MacDonald, Lamprini Veneti, Tine Ravlo, Heidi Lange,
504 Umaer Naseer, Siri Feruglio, Karoline Bragstad, Olav Hungnes, Liz E Ødeskaug,
505 et al. Outbreak caused by the SARS-CoV-2 Omicron variant in Norway, Novem-
506 ber to December 2021. *Eurosurveillance*, 26(50):2101147, 2021.
- 507 [23] James A Hay, Stephen M Kissler, Joseph R Fauver, Christina Mack, Caroline G
508 Tai, Radhika M Samant, Sarah Connelly, Deverick J Anderson, Gaurav Khullar,
509 Matthew MacKay, et al. Viral dynamics and duration of PCR positivity of the
510 SARS-CoV-2 Omicron variant. *medRxiv*, 2022.
- 511 [24] Carl AB Pearson, Sheetal P Silal, Michael WZ Li, Jonathan Dushoff, Ben-
512 jamin M Bolker, Sam Abbott, Cari van Schalkwyk, Nicholas G Davies,
513 Rosanna C Barnard, W John Edmunds, et al. Bounding the levels of trans-
514 missibility & immune evasion of the Omicron variant in South Africa. *MedRxiv*,
515 2021.
- 516 [25] Sang Woo Park, Benjamin M Bolker, Sebastian Funk, C Jessica E Metcalf,
517 Joshua S Weitz, Bryan T Grenfell, and Jonathan Dushoff. Roles of generation-
518 interval distributions in shaping relative epidemic strength, speed, and control
519 of new SARS-CoV-2 variants. *medRxiv*, 2021.
- 520 [26] Moritz UG Kraemer, Oliver G Pybus, Christophe Fraser, Simon Cauchemez,
521 Andrew Rambaut, and Benjamin J Cowling. Monitoring key epidemiological
522 parameters of SARS-CoV-2 transmission. *Nature medicine*, 27(11):1854–1855,
523 2021.
- 524 [27] Sang Woo Park, Daniel M Cornforth, Jonathan Dushoff, and Joshua S Weitz.
525 The time scale of asymptomatic transmission affects estimates of epidemic po-
526 tential in the COVID-19 outbreak. *Epidemics*, 31:100392, 2020.